ELSEVIER

Chemistry & Biology 8 (2001) 857–870

Chemistry & Biology

www.elsevier.com/locate/chembiol

Research Paper

Minimization of MC1R selectivity by modification of the core structure of α-MSH-ND

Sung-Kil Lim [a,1,*], Song-Zhe Li [a,1], Chang-Hun Lee [b], Chang-Ju Yoon [c], Ja-Hyun Baik [d], Weontae Lee [b]

[a] *Division of Endocrinology, Department of Internal Medicine, College of Medicine, Yonsei University, 134 Shinchon-Dong, Seodaemoon-Gu, 120-752 Seoul, South Korea*

[b] *Department of Biochemistry, College of Science, Yonsei University, 134 Shinchon-Dong, Seodaemoon-Gu, 120-749 Seoul, South Korea*

[c] *Department of Chemistry, College of Science, Catholic University, 43-1 Yokmoo-Dong Wonmi-Gu, 420-743 Puchon City, South Korea*

[d] *Laboratory of Molecular Biology, Medical Research Center, College of Medicine, Yonsei University, 134 Shinchon-Dong, Seodaemoon-Gu, 120-752 Seoul, South Korea*

Received 30 November 2000; revisions requested 7 February 2001; revisions received 28 May 2001; accepted 18 June 2001
First published online: 12 July 2001

Abstract

Background: Melanocortin, through its distinct receptor subtypes, has many different effects. Receptor-selective ligands are required to reduce the undesirable effects of melanocortin. To investigate which conformation is preferable to a given melanocortin receptor subtype, a structural and functional analysis of the ligand–receptor interactions was made by studying the biological activity, the nuclear magnetic resonance structures, and the patterns of the ligand–receptor interaction for each receptor subtype by homology modeling analysis.

Results: Among the several analogues examined, [Gln^6]α-melanocyte-stimulating hormone (MSH)-ND was found to have 10 000 times less biological activity than α-MSH-ND for the MC1R, whereas, the potencies of both oligopeptides were comparable in both the melanocortin-3 receptor (MC3R) and MC4R. [Gln^6]α-MSH-ND exhibited a type I′ β-turn that was similar to the type I β-turn structure of α-MSH-ND. However, a remarkable structural difference was observed with respect to the side chain orientations of the sixth and seventh residues of [Gln^6]α-MSH-ND, which were found to be mirror images of α-MSH-ND. By homology modeling analysis, the His^6 of α-MSH-ND was found to interact with the TM2 regions of all three receptors (Glu^{94} of MC1R, Glu^{94} of MC3R, and Glu^{100} of MC4R), but [Gln^6]α-MSH-ND did not. The phenyl ring of the D-Phe^7 residue of [Gln^6]α-MSH-ND revealed an interaction with the TM3 regions of both the MC3R and MC4R (Ser^{122} of MC3R or Ser^{127} of MC4R). However, in the MC1R, these serine residues corresponded to Val^{122}, which contains two methyl groups that induce steric hindrance with D-Phe^7 of [Gln^6]α-MSH-ND. This is a possible explanation for the biological activity of [Gln^6]α-MSH-ND for the MC1R being significantly lower than that for either the MC3R or MC4R.

Conclusions: Minimization of the MC1R selectivity whilst preserving its comparable potency for both the MC3R and MC4R could be achieved by modifying the D-Phe^7 orientation of α-MSH-ND, while maintaining the 'type I β-turn'-like structure.

Keywords: Melanocortin receptor; Binding affinity; cAMP-generating activity; Nuclear magnetic resonance; Type I β-turn; Homology modeling

Abbreviations: MC1R, melanocortin-1 receptor; MC3R, melanocortin-3 receptor; MC4R, melanocortin-4 receptor; MSH, melanocyte-stimulating hormone; Ahx, α-aminohexanoic acid; CHO, Chinese hamster ovary cell line; NMR, nuclear magnetic resonance; REM, restraints energy minimization; TOCSY, total correlation spectroscopy; ROESY, rotating-frame Overhauser effect spectroscopy; NOESY, nuclear Overhauser effect spectroscopy; DG, distance geometry; DQF-COSY, double-quantum-filtered correlated spectroscopy; TM, transmembrane

[1] These two authors contributed equally to this work.

* Corresponding author.
E-mail addresses: lsk@yumc.yonsei.ac.kr (S.-K. Lim), cjyoon@www.cuk.ac.kr (C.-J. Yoon), jahyunb@yumc.yonsei.ac.kr (J.-H. Baik), wlee@nestis.yonsei.ac.kr (W. Lee).

1074-5521/01/$ – see front matter
PII: S1074-5521(01)00057-6

1. Introduction

Melanocortins, including α-melanocyte-stimulating hormone (MSH) have been implicated in a variety of physiologic functions, such as skin pigmentation, learning, memory, analgesic and anti-inflammatory effects, the regulation of blood pressure, immune modulation and food intake [1–6]. The cloning of five melanocortin receptor subtypes has facilitated research in this field and provided the tools for a systematic study of the molecular mechanisms involved in the physiologic effects of these subtypes [7–13]. As melanocortin has many different effects related to the distinct receptor subtypes, a selective ligand for a given receptor subtype is required to reduce its undesirable effects. Hence, the structural and functional analysis of the ligand–receptor interactions of melanocortin has assumed greater importance.

In a previous nuclear magnetic resonance (NMR) study [14], it was shown that the core residues of His^6-(D-Phe) ^{7}-Arg^8-Trp^9 of α-MSH-ND formed a stable structure called the type I β-turn, and that substitution of the His^6 residue with other amino acid residues resulted in remarkable structural changes. The receptor binding affinity and the cAMP-generating activity of the substitutes at both the MC3R and MC4R were also significantly decreased. Therefore, it is proposed in this study that the structure of the type I β-turn, which is composed of core residues, might be important for α-MSH analogues both to bind optimally with and to activate both the MC3R and MC4R [15].

The selectivity and biological potency of a diverse number of peptides have been determined in terms of the peptide backbone structure and its side chains [16–21]. Haskell-Luevano et al. incorporated a methyl group on the β-carbons of the two aromatic amino acids to identify the 3D orientation of the Phe^7 and Trp^9 amino acids when binding to melanocortin-1 receptor (MC1R). They found that the 3D orientation of these amino acids can affect both the potencies and the prolonged biological activities of melanotropin peptides [22]. However, they did not show how the side chain orientations of the melanocortin pharmacophores affect the ligand–receptor interactions and biological activity.

In a previous NMR study, [Gln^6]α-MSH-ND was found to have a similar backbone structure to the type I β-turn of α-MSH-ND, the so-called type I′ β-turn. In contrast, the side chains of the sixth and seventh residues of [Gln^6]α-MSH-ND were mirror images of the respective α-MSH-ND residues. The biological potency of [Gln^6]α-MSH-ND for MC1R was significantly lower than that of α-MSH-ND. However, this was not the case for either the MC3R or the MC4R. These findings imply that differences in the side chain orientation of both oligopeptides, which show isomeric conformations, can have a remarkable affect on the biological potency according to receptor subtype. This study aimed to determining how melanocortin interacts with a given receptor subtype, and how the differences in the side chain orientation affect selectivity. This was accomplished by combining the NMR structural characteristics, the receptor binding affinities, and the cAMP-generating activity of both α-MSH-ND and [Gln^6]α-MSH-ND, with the results obtained from the receptor homology modeling analysis results.

2. Results

To investigate the relationship between the structure and function of the melanocortins, several α-MSH analogues were synthesized (Table 1), and their biological activities were tested. In addition, an attempt was made to further understand their structural characteristics and the possible structural features of the melanocortin receptor subtypes based upon their ligand–receptor interactions.

2.1. Receptor binding activity of α-MSH analogues

The [α-aminohexanoic acid (Ahx)^4]α-MSH, NDP-MSH

Table 1
Sequences of the α-MSH analogues used in this study

Peptides	Position												
	1	2	3	4	5	6	7	8	9	10	11	12	13
[Ahx^4]α-MSH	Ser	Tyr	Ser	Ahx	Glu	His	Phe	Arg	Trp	Gly	Lys	Pro	Val
NDP-MSH	Ser	Tyr	Ser	Ahx	Glu	His	D-Phe	Arg	Trp	Gly	Lys	Pro	Val
α-MSH-ND				Ahx	Asp	His	D-Phe	Arg	Trp	Lys			
[Gln^6]α-MSH-ND				Ahx	Asp	*Gln*	D-Phe	Arg	Trp	Lys			
[Trp^6]α-MSH-ND				Ahx	Asp	*Trp*	D-Phe	Arg	Trp	Lys			
[Asn^6]α-MSH-ND				Ahx	Asp	*Asn*	D-Phe	Arg	Trp	Lys			
[Arg^6]α-MSH-ND				Ahx	Asp	*Arg*	D-Phe	Arg	Trp	Lys			
[Lys^6]α-MSH-ND				Ahx	Asp	*Lys*	D-Phe	Arg	Trp	Lys			
[Tyr^6]α-MSH-ND				Ahx	Asp	*Tyr*	D-Phe	Arg	Trp	Lys			
[Trp6]α-MSH-ND(6–10)						*Trp*	D-Phe	Arg	Trp	Lys			
[Trp^6]α-MSH-ND(6–9)						*Trp*	D-Phe	Arg	Trp				

All peptides have an acetyl-group on the N-terminus and an amide group on the C-terminus. The main substituted amino acid residues are shown in italics.

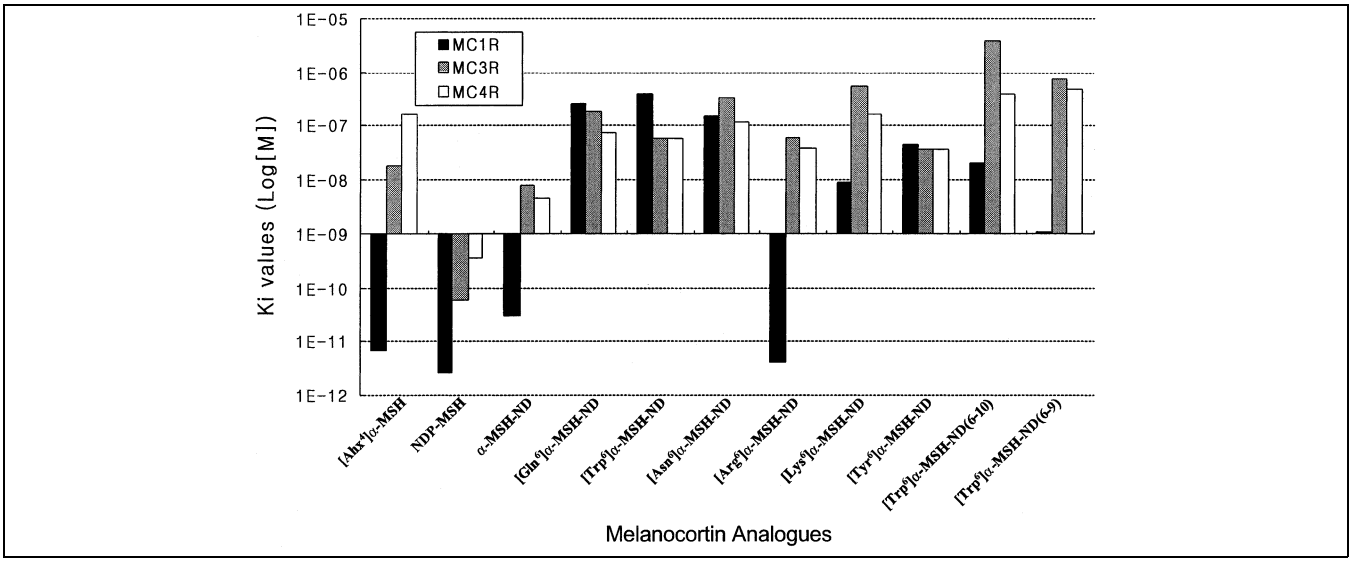

Fig. 1. Receptor binding affinities of the different α-MSH analogues. The CHO cells over-expressing MC1R, MC3R or MC4R were incubated with a fixed concentration of ~2 nM ^{125}I-labelled NDP-MSH in the presence of increasing concentrations of α-MSH analogues as indicated. The ordinate represents the mean K_i values, which were determined using a software package suitable for radioligand binding analysis (GraphPad Prism Program).

and α-MSH-ND binding affinities for the MC1R were measured to determine the roles of the seventh residue in the receptor–ligand interaction. As shown in Table 2, the order of preference was NDP-MSH > [Ahx^4]α-MSH > α-MSH-ND. Their K_i values (nM) at the MC1R were 0.0026 ± 0.0019, 0.0068 ± 0.0011 and 0.0314 ± 0.0198, respectively. A comparison of the binding affinities of the three analogues revealed a preference for the MC1R as opposed to the MC3R and MC4R (Fig. 1). Substitution of the seventh residue, from Phe to D-Phe, induced a remarkably potentiated selectivity for MC4R. Even though α-MSH-ND did not show a higher binding affinity than [Ahx^4]α-MSH as was detected for both the MC3R and MC4R, it still bound to the MC1R quite well.

When the α-MSH-ND His^6 residue was substituted with Gln, Trp, Asn, Arg, Lys or Tyr, as shown in Fig. 1, all the analogues with the exception of [Arg^6]α-MSH-ND showed a significantly decreased binding affinity for the MC1R. The order of their MC1R binding affinities were: [Arg^6]α-MSH-ND > α-MSH-ND ≫ [Lys^6]α-MSH-ND > [Tyr^6]α-MSH-ND > [Asn^6]α-MSH-ND > [Gln^6]α-MSH-ND > [Trp^6]α-MSH-ND, and their K_i values (nM) were 0.0041 ± 0.0014, 0.0314 ± 0.0198, 8.828 ± 3.362, 43.87 ± 16.68, 151.38 ± 20.78, 243.33 ± 29.83 and 392.01 ± 165.70, respectively. In addition, the K_i values of the two additionally synthesized peptides, [Trp^6]α-MSH-ND and [Tyr^6]α-MSH-ND, were 57.25 ± 11.59 and 36.24 ± 5.22, respectively, at the MC3R, but 57.60 ± 20.03 and 36.07 ± 6.957, respectively, at the MC4R. From the observed binding affinities of these receptors, it was found that, with the exception of Arg, the replacement of His^6 with the other residues resulted in a 10 000-fold decrease in the binding affinity for the MC1R, while a reasonable binding activity was still maintained for both the MC3R

Table 2
K_i values (mean ± S.E.M.) of the α-MSH analogues obtained from a computer analysis of the competition curves on the stable transfected CHO cells over-expressing MC1R, MC3R or MC4R

Ligands	K_i (nM)		
	MC1R	MC3R	MC4R
[Ahx^4]α-MSH	0.0068 ± 0.0011	17.64 ± 5.33	156.69 ± 20.04
NDP-MSH	0.0026 ± 0.0019	0.061 ± 0.012	0.372 ± 0.128
α-MSH-ND	0.0314 ± 0.0198	7.801 ± 1.501	4.405 ± 0.704
[Gln^6]α-MSH-ND	243.33 ± 29.83	177.51 ± 19.84	73.64 ± 17.06
[Trp^6]α-MSH-ND	392.01 ± 165.70	57.25 ± 11.59	57.60 ± 20.03
[Asn^6]α-MSH-ND	151.38 ± 20.78	330.22 ± 60.05	112.57 ± 9.738
[Arg^6]α-MSH-ND	0.0041 ± 0.0014	59.75 ± 9.54	37.74 ± 5.504
[Lys^6]α-MSH-ND	8.828 ± 3.362	552.02 ± 144.96	156.56 ± 26.72
[Tyr^6]α-MSH-ND	43.87 ± 16.68	36.24 ± 5.22	36.07 ± 6.957
[Trp^6]α-MSH-ND(6–10)	20.04 ± 4.473	3,837.7 ± 1,486.8	396.82 ± 107.77
[Trp^6]α-MSH-ND(6–9)	1.099 ± 0.426	728.37 ± 333.66	490.98 ± 55.93

Table 3
EC_{50} values (mean ± S.E.M.) of the α-MSH analogues obtained from a computer analysis of the dose–response curves on the stably transfected CHO cells over-expressing MC1R, MC3R or MC4R

Ligands	EC_{50}(nM)		
	MC1R	MC3R	MC4R
[Ahx^4]α-MSH	0.00558 ± 0.00131	9.362 ± 1.932	46.040 ± 0.020
NDP-MSH	0.00067 ± 0.00039	0.174 ± 0.052	0.126 ± 0.020
α-MSH-ND	0.00799 ± 0.00451	1.523 ± 0.707	0.780 ± 0.405
[Gln^6]α-MSH-ND	96.62 ± 32.276	9.383 ± 4.620	7.880 ± 1.818
[Trp^6]α-MSH-ND	387.9 ± 164.10	110.00 ± 35.701	*0.812 ± 0.428*
[Asn^6]α-MSH-ND	16.77 ± 6.944	271.80 ± 21.948	*0.799 ± 0.121*
[Arg^6]α-MSH-ND	1.765 ± 0.800	0.381 ± 0.157	4.858 ± 0.949
[Lys^6]α-MSH-ND	6.879 ± 2.650	29.560 ± 11.525	19.890 ± 4.024
[Tyr^6]α-MSH-ND	178.8 ± 45.269	76.860 ± 12.088	273.60 ± 259.668
[Trp^6]α-MSH-ND(6–10)	*1795 ± 189*	—	184.80 ± 110.625
[Trp^6]α-MSH-ND(6–9)	512.40 ± 64.68	—	11.320 ± 8.957

The values in italics mean that their mature cAMP generation failed to reach the maximum stimulation as shown by other analogues.
'—' indicates that the compounds did not show the visible effect on cAMP-generation even at the highest concentration used in this experiments.

and MC4R. Fig. 3A shows that the [Gln^6]α-MSH-ND-binding activity for the MC1R was substantially lower than that of α-MSH-ND. However, this was not the case in terms of its relative binding affinities for either the MC3R or the MC4R.

[Trp^6]α-MSH-ND showed the lowest binding activity for the MC1R. To further investigate whether or not the shorter analogues could have biological activity, two peptides, [Trp^6]α-MSH-ND(6–10) and [Trp^6]α-MSH-ND(6–9), were synthesized by deleting either both the Ahx^4 and Asp^5 residues only or by deleting them together with Lys^{10}. Their binding affinities for the MC1R, MC3R and MC4R were determined. As shown in Table 2, [Trp^6]α-MSH-ND(6–10) and [Trp^6]α-MSH-ND(6–9) showed K_i values (nM) of 20.04 ± 4.473 and 1.099 ± 0.426, respectively, for the MC1R, 3837.7 ± 1486.8 and 728.37 ± 333.66, respectively, for the MC3R, and 396.82 ± 107.77 and 490.98 ± 55.93, respectively, for the MC4R. Compared with [Trp^6]α-MSH-ND, the truncated peptides showed significantly lower binding affinities for both the MC3R and MC4R (Fig. 1). The order of preference for the MC3R was [Trp^6]α-MSH-ND > [Trp^6]α-MSH-ND(6–9) > [Trp^6]α-MSH-ND-(6–10), and for the MC4R, [Trp^6]α-MSH-ND > [Trp^6]α-MSH-ND(6–10) > [Trp^6]α-MSH-ND(6–9). However, [Trp^6]α-MSH-ND(6–9) exhibited a higher binding activity than [Trp^6]α-MSH-ND for the MC1R with an order of preference of [Trp^6]α-MSH-ND(6–9) > [Trp^6]α-MSH-ND(6–10) > [Trp^6]α-MSH-ND. These results suggested that the shorter analogue, despite being composed of

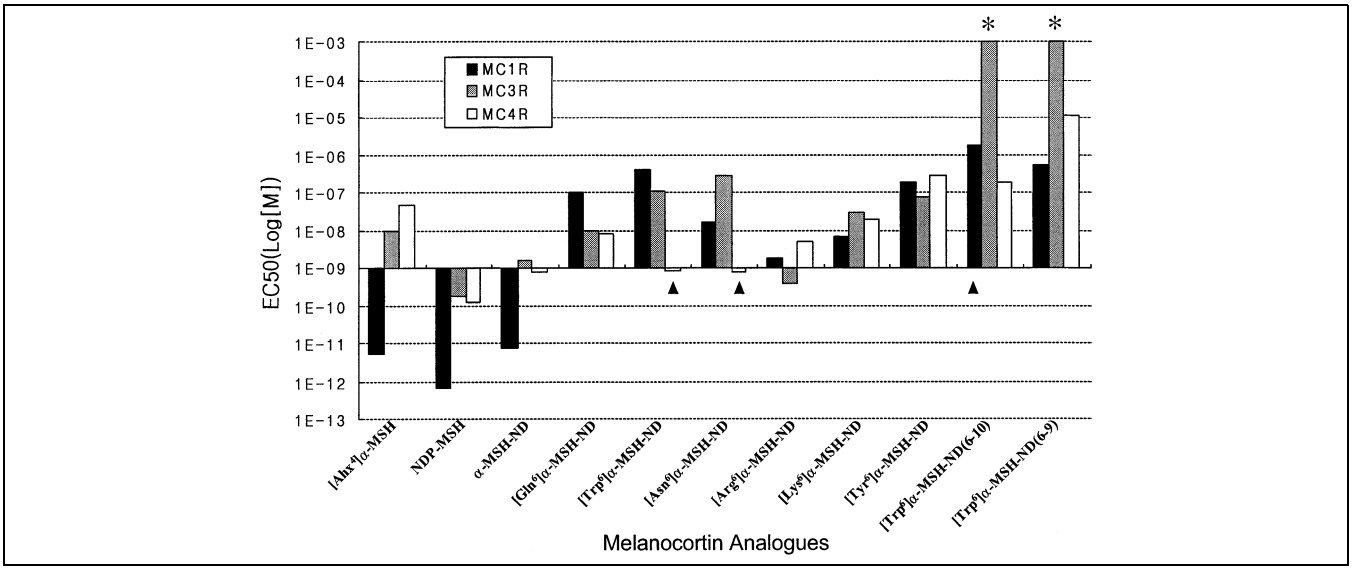

Fig. 2. cAMP-generating activity of different α-MSH analogues. The potencies of the α-MSH analogues are shown as the mean EC_{50} values. The bars indicated with '▲' show that mature cAMP generation failed to reach the maximum stimulation level shown by other analogues. '*' indicates that the analogues did not exhibit a significant effect on cAMP generation even at the highest concentrations indicated.

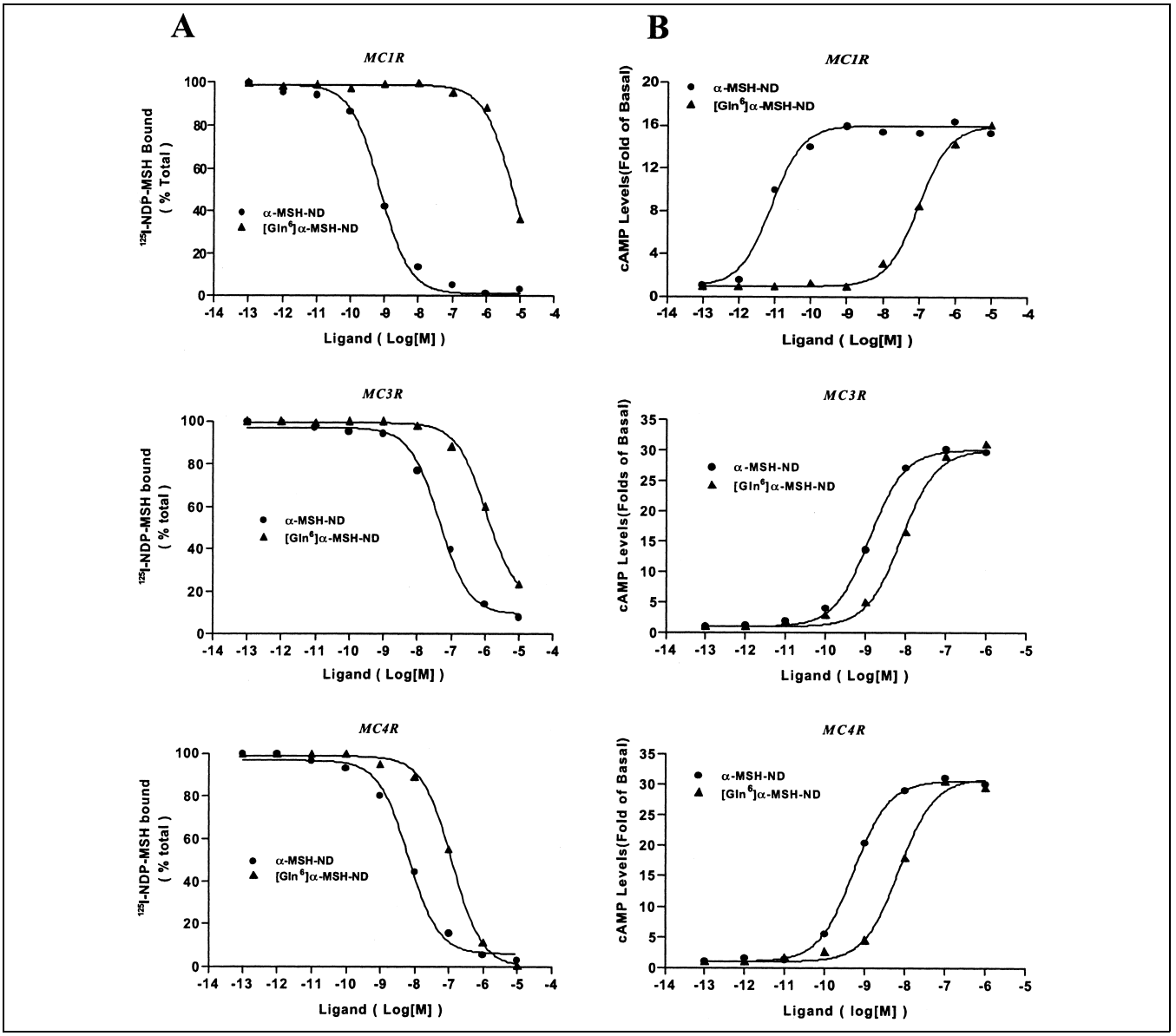

Fig. 3. Comparison of the biological activities of α-MSH-ND (●) and [Gln^6]α-MSH-ND (▲) at MC1R, MC3R and MC4R. (A) Competition binding. The CHO cells over-expressing MC1R, MC3R or MC4R were incubated with a fixed concentration of ~2 nM ^{125}I-labelled NDP-MSH in the presence of increasing concentrations of either α-MSH-ND or [Gln^6]α-MSH-ND as indicated. The ordinate represents the percentage of the total specific binding (B_{max}). The curves were fitted using non-linear regression analysis and a one-site competition model (GraphPad Prism). (B) cAMP-generating activity assay. The cells stably transfected with MC1R, MC3R or MC4R were treated with various concentrations of α-MSH-ND or [Gln^6]α-MSH-ND, and the intracellular cAMP production was assayed. The ordinate shows folds of the basal (indicated as 10^{-13} M) cAMP level obtained for each curve. The curves were fitted using the sigmoidal dose–response model with a variable slope factor (GraphPad Prism). All curves are representative of two independent experiments, and each point represents the mean of three values.

only four core residues, is still capable of generating a binding affinity for the MC1R.

2.2. *Effects of α-MSH analogues on cAMP accumulation in Chinese hamster ovary (CHO) cells over-expressing MC1R, MC3R or MC4R*

In a manner identical to the binding assay results described above, [Ahx^4]α-MSH, NDP-MSH and α-MSH-ND at the MC1R exhibited cAMP-generating activities in the order NDP-MSH > [Ahx^4]α-MSH > α-MSH-ND (Fig. 2); their corresponding EC_{50} values (nM) for the MC1R were 0.00558 ± 0.00131, 0.00067 ± 0.00039 and 0.00799 ± 0.00451, respectively (Table 3). Compared with their cAMP stimulation at both the MC3R and MC4R, all these three analogues showed higher biological activity at the MC1R, which is consistent with the results of the binding assay.

Substituting His^6 for either Gln, Trp, Asn, Arg, Lys or Tyr brought about reductions in cAMP accumulations,

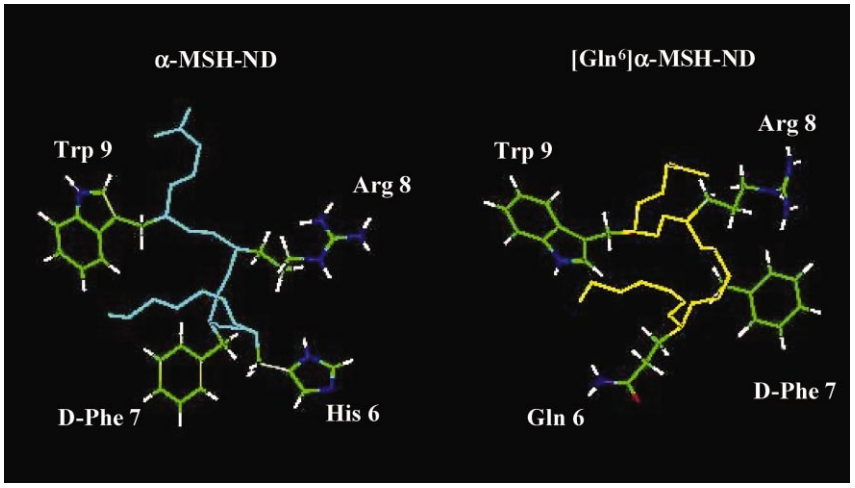

Fig. 4. Structural comparison of two MSH analogues, α-MSH-ND and [Gln^6]α-MSH-ND. The solution structures of α-MSH-ND and [Gln^6]α-MSH-ND, as determined by NMR, were aligned for the primary sequences so that the corresponding residues of each peptide were located in the same orientation.

especially at the MC1R. Their potencies at the MC1R were in the order: α-MSH-ND ≫ [Arg^6]α-MSH-ND > [Lys^6]α-MSH-ND > [Asn^6]α-MSH-ND > [Gln^6]α-MSH-ND > [Tyr^6]α-MSH-ND > [Trp^6]α-MSH-ND, and the corresponding EC_{50} values (nM) were 0.00799 ± 0.00451, 1.765 ± 0.800, 6.879 ± 2.650, 16.77 ± 6.944, 96.62 ± 32.276, 178.8 ± 45.269 and 387.9 ± 164.10, respectively (Table 3). Analogues with positively charged residues at the sixth position, such as His^6, Arg^6 and Lys^6, produced higher cAMP-generating activities than the others. Specifically, [Gln^6]α-MSH-ND showed a 10 000-fold reduction in cAMP-generating activity at the MC1R, which was more significant than that observed at either the MC3R or the MC4R (Fig. 3B). In addition, [Tyr^6]α-MSH-ND exhibited EC_{50} values of 76.860 ± 12.088 at the MC3R, and 273.60 ± 259.668 at the MC4R. The two truncated forms, [Trp^6]α-MSH-ND(6–10) and [Trp^6]α-MSH-ND(6–9), did not show any cAMP-generating activity at the MC3R, with the former yielding an EC_{50} value (nM) of 184.80 ± 110.625 at the MC4R and the latter 512.40 ± 64.68 at the MC1R.

2.3. Solution structures of α-MSH analogues

The restraints energy minimization (REM) average structures of the α-MSH analogues for receptor–ligand complex modeling were calculated from the NMR structures based on the reported data [14,15]. Even though these ligand structures were derived in the free state, they were able to explain the key features of the binding affinity because the more adaptable a ligand structure is, the greater the likelihood that it can initiate receptor binding. To compare the backbone conformations of [Gln^6]α-MSH-ND and α-MSH-ND, the REM structure of [Gln^6]α-MSH-ND was superimposed, with specific attention placed on the Asp^5 to Arg^8 residues of α-MSH-ND. As shown in Fig. 4, the solution structures of α-MSH-ND and [Gln^6]α-MSH-ND were aligned for the primary sequences in order that the corresponding peptides residues would be located in the same orientation. It was found that the side chains of the center residues of the β-turn, His^6 and D-Phe^7 of α-MSH-ND, and the Gln^6 and D-Phe^7 of [Gln^6]α-MSH-ND, have an opposing orientation, whereas, the Arg^8 and Trp^9 orientations were similar. This demonstrates that the sixth and seventh residues of [Gln^6]α-MSH-ND have a mirror image conformation relative to α-MSH-ND. In addition, the solution structure of α-MSH-ND demonstrates a type I β-turn composed of Asp^5, His^6, D-Phe^7 and Arg^8, while [Gln^6]α-MSH-ND exhibits a type I′ β-turn structure comprised of Asp^5, Gln^6, D-Phe^7 and Arg^8.

2.4. Receptor–ligand interactions analyzed by homology modeling

A putative ligand binding model for the receptor was constructed by docking the NMR structures of the MSH analogues with each type of melanocortin receptor model based on both the mutagenetic data and homology modeling. Most of the results obtained from the mutagenetic studies [23–25] were clearly explained by this model. In this homology modeling study, the polar side chain of His^6 in α-MSH-ND was found to interact, as shown in Fig. 5, with the transmembrane (TM)2 domains of the melanocortin receptors, namely Glu^{94} of the MC1R, Glu^{94} of the MC3R and Glu^{100} of the MC4R. Simultaneously, the Arg^8 residue of this ligand demonstrated an interaction with the Asp^{121} residues of the MC1R (Fig. 5A), the Asp^{121} of the MC3R (Fig. 5B) and the Asp^{126} of the MC4R (Fig. 5C). Exchanging the sixth residue of α-MSH-ND to Gln from His^6, to form [Gln^6]α-MSH-ND, resulted in a mirror image with an altered orientation of

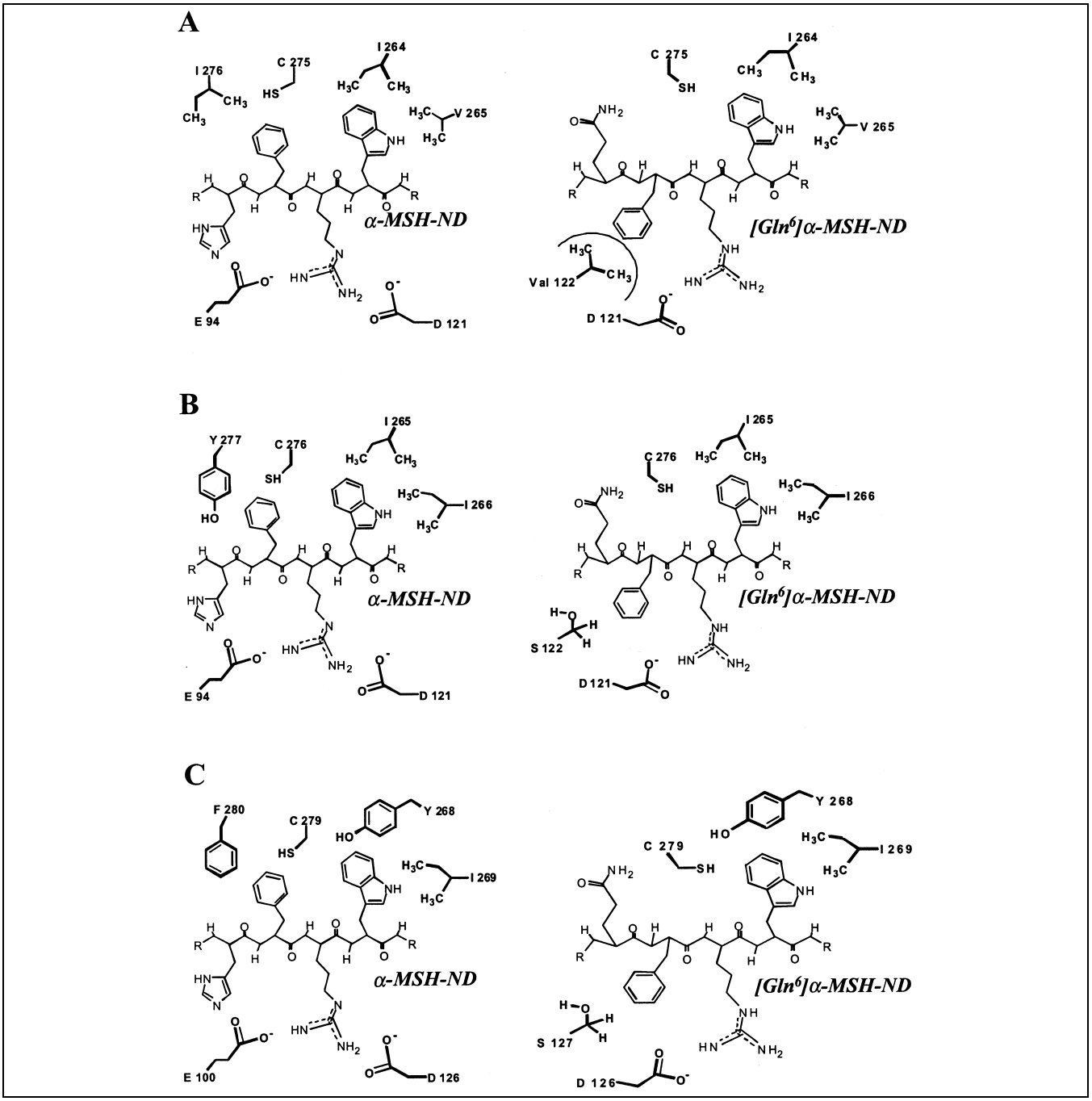

Fig. 5. Schematic diagram of the ligand–receptor binding model. The possible interactions between ligands and receptors were elucidated from the complex structures determined by the NMR ligand structure and the homology models of MC1R, MC3R, and MC4R in alphabetical order, A, B, and C, respectively. The structures of both α-MSH-ND and [Gln^6]α-MSH-ND are displayed by thin lines, whereas the receptor residues are displayed by thick lines.

the sixth and seventh residues. Since the direction of the Gln^6 residue side chain differed from that of His^6, it could not interact with the TM2 domains of all of the receptors, whereas the Arg^8 residue of [Gln^6]α-MSH-ND maintained the same level of interaction as α-MSH-ND.

The phenyl ring of α-MSH-ND interacted with both the Cys^{275} and Ile^{276} of the MC1R, both the Cys^{276} and Tyr^{277} of the MC3R, and both the Cys^{279} and Phe^{280} of the MC4R. These all belong to the TM7 region of each receptor. However, D-Phe^7 of [Gln^6]α-MSH-ND could not interact with any of these residues. Instead, as shown in Fig. 5B,C, it adjoined the residues of the TM3 domains, either Ser^{122} of the MC3R or Ser^{127} of the MC4R. Moreover, the serine residues of both the MC3R and MC4R correspond to Val^{122} of the MC1R (Fig. 5A), which contains a non-polar side chain with two methyl groups. It is noteworthy that the important residues in the hydrophobic binding pockets of the MC1R were clearly different

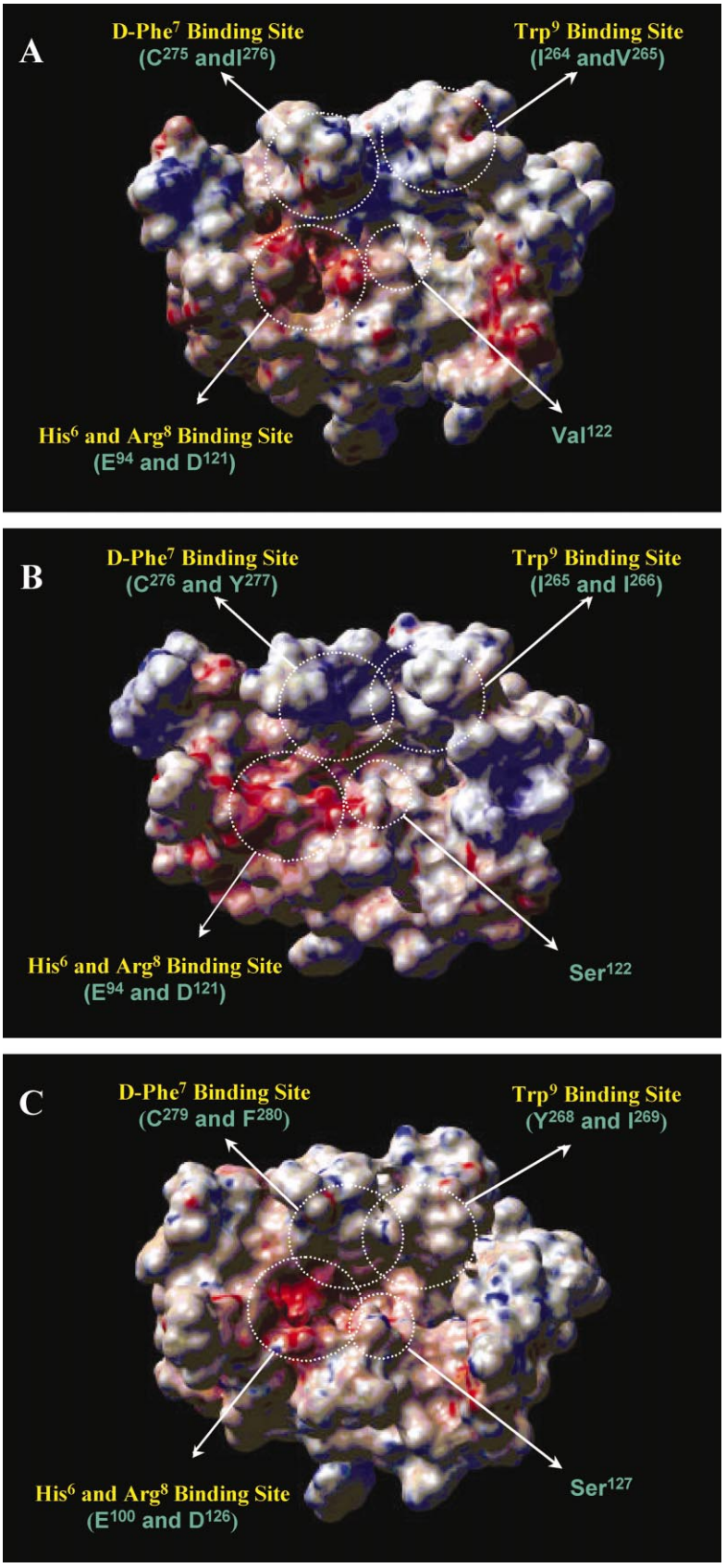

Fig. 6. Stereo-view of the homology models for each subtype of the melanocortin receptors. The calculated MC1R, MC3R, and MC4R models are demonstrated in A, B, and C, respectively. To show the binding cavities clearly, N-terminal regions, exoloops and cytosolic loops have been omitted. The characters in yellow show ligand residues, and those in green represent receptor residues.

from those of the other receptors. The Ile^{276} residue of the MC1R (Fig. 5A), which is involved in the D-Phe^{7} binding site, mutated to Tyr^{277} in the MC3R (Fig. 5B) and Phe^{280} in the MC4R (Fig. 5C). On the other hand, the residues of each receptor at the Trp^{9} binding cavity lying in the TM6 domains, either Ile^{264} of the MC1R (Fig. 5A) or Ile^{265} of the MC3R (Fig. 5B), were replaced with Tyr^{268} in the MC4R (Fig. 5C). Val^{265} in the MC1R (Fig. 5A), the other residue interacting with Trp^{9}, was substituted for Ile^{266} in the MC3R and Ile^{269} in the MC4R (Fig. 5C). Overall, as shown in Fig. 6, all these changes can cause the binding pocket of the MC4R to be narrower than that of either the MC1R or the MC3R.

Although the models constructed in this study showed distinct ligand binding patterns in the three receptors, they indicated that the TM2, TM3, TM6 and TM7 segments of these receptors participate in the formation of the binding pocket for the core sequence of the α-MSH analogues. These structures are well supported by mutagenetic data, which demonstrates that TM4 and TM5 are not involved in ligand binding [26]. Apart from the residues mentioned above, the effects of other important residues on ligand binding were also investigated. For example, both Phe^{258} and His^{260} in the TM6 segment of the MC1R did not appear to be involved in the direct ligand interaction, but rather to be located close to the Trp^{9} residue of the core sequence. This indicates that subtle changes of the local structure at Phe^{258} and His^{260} can also influence ligand binding or receptor activation. Moreover, the Asn^{277} residues of the MC1R, the His^{280} residues of the MC3R and the His^{283} residues of the MC4R were found to occur at the bottom of the binding pockets. Furthermore, all of these residues can operate as hydrogen donors or as acceptors for hydrogen bonding. Therefore, it is possible that these residues determine the specificity for ligand binding by forming hydrogen bonds with backbone amide hydrogen or carbonyl oxygen. The prerequisite characteristic of a type I β-turn structure may be closely related to these Asn or His residues.

3. Discussion

By cloning the five different melanocortin receptors, the mechanisms of many known physiologic functions of melanocortins were elucidated. These include central effects such as the control of motor and sexual behavior, analgesia, memory improvement, and antipyretic effects, as well as peripheral effects, such as powerful anti-inflammatory and lipolytic effects. As the melanocortins reveal so many different effects through their distinct receptor subtypes, selective ligands for the given receptor subtypes are required in order to reduce the undesirable effects of melanocortin. Therefore, structural and functional analyses based on the interaction between the melanocortin analogues and different melanocortin receptor subtypes are important, and will provide valuable information for structure-based drug design.

In a previous study, the authors reported that [Ahx^{4}]α-MSH showed a loop structure, while NDP-MSH exhibited a 'type I β-turn'-like structure (data unpublished). The structural change from [Ahx^{4}]α-MSH to NDP-MSH remarkably enhanced both the receptor binding affinity and the cAMP-generating activity at the MC1R, MC3R and MC4R. This result indicated that changes towards a conformation resembling the type I β-turn could bring about augmented biological activity in these receptors. Compared to NDP-MSH, the potency of α-MSH-ND was relatively weak at all three melanocortin receptors, which suggests that the residues at the C-terminus of NDP-MSH are important for enhancing ligand potency to the MC1R, MC3R and MC4R.

Substitution of the α-MSH-ND His^{6} residue by Gln, Trp, Asn, Lys or Tyr resulted in a remarkable reduction in biological activity. Compared to the MC3R and MC4R, most of the α-MSH analogues, with the exception of [Arg^{6}]α-MSH-ND, exhibited significant decreases in terms of their binding affinities to the MC1R. With regard to the cAMP-generating activity, those analogues containing a positively charged residue at the sixth position, such as α-MSH-ND, [Arg^{6}]α-MSH-ND and [Lys^{6}]α-MSH-ND, showed relatively high cAMP-generating activities at all three receptors. These results suggest that the sixth residue plays an important role in activating the MC1R, MC3R and MC4R, and that there is probably some charge interaction between the sixth residue of α-MSH-ND and the three receptors. This is supported by homology modeling analysis, which suggests that the α-MSH-ND His^{6} residue probably interacts with the TM2 Glu residues in all these receptors (Fig. 5).

α-MSH-ND revealed a tight type I β-turn conformation, while [Gln^{6}]α-MSH-ND showed a similar structure to the type I β-turn of α-MSH-ND, the so-called 'type I′ β-turn' structure. Even though this difference in backbone structure is very subtle, [Gln^{6}]α-MSH-ND showed an approximate 10 000-fold reduction in biological activity compared to α-MSH-ND at the MC1R, while the biological potency of both oligopeptides was comparable to that at both the MC3R and MC4R. In a previous study [15], both [Lys^{6}]α-MSH-ND and [Gln^{6}]α-MSH-ND(6–10) were shown to have γ-turn conformations and both of them were found to have reduced receptor binding and cAMP-generating activity at the MC1R. Therefore, the more the structure of an α-MSH-ND-derived analogue diverges from the type I β-turn, the less its preference for the MC1R. However, using homology modeling analysis, it was found that the binding pocket of the MC1R was much broader than that of the MC4R (Fig. 6). This indicates that the MC1R might be significantly more tolerant to subtle changes in ligand conformation. However, [Gln^{6}]α-MSH-ND could not activate this receptor effectively. Therefore, subtle differences in the backbone struc-

ture alone cannot explain the different biological potency of [Gln^6]α-MSH-ND at the MC1R.

The selectivity or biological potencies of a diverse number of peptides have been examined both in terms of their backbone structures and their side chain characteristics [16–21]. The backbone structures of α-MSH-ND and [Gln^6]α-MSH-ND are quite similar, whereas their side chain orientations are different and it was determined that [Gln^6]α-MSH-ND is a mirror image analogue of α-MSH-ND. To define how such conformational differences could result in such great differences in biological activity at the MC1R, this study compared their individual binding patterns to these receptors. Molecular modeling analysis revealed that the positively charged His^6 residue of α-MSH-ND interacts with the negatively charged Glu residues in the TM2 regions of the three melanocortin receptors, whereas the Gln^6 in [Gln^6]α-MSH-ND does not (Fig. 5). This indicates that the alteration in the latter's side chain orientation, which lacks a charge interaction with the TM2 regions, is responsible for the significant reduction in biological activity at these receptors. Hydrophobic binding pockets in each receptor are composed of diverse hydrophobic amino acids, which may also confer binding activity or specificity. NMR analysis revealed that the D-Phe^7 residue of [Gln^6]α-MSH-ND to be a mirror image of the corresponding α-MSH-ND position. This directional displacement changed the D-Phe^7 binding sites of all receptors from the hydrophobic binding domain of the TM7 region to that of the TM3 regions as shown in Fig. 5. Therefore, the altered receptor binding patterns of the [Gln^6]α-MSH-ND D-Phe^7 residues may also explain the decreased biological potency at all the receptors.

None of the TM2 regions in any of the three receptor subtypes would bind to [Gln^6]α-MSH-ND, because of the altered orientation of Gln^6. However, the Arg^8 and Trp^9 binding sites of all three receptors exhibited similar binding. Therefore, the changed D-Phe^7 orientation in [Gln^6]α-MSH-ND was considered to be most likely responsible for the significant decrease in biological activity at the MC1R, while such a change was tolerable at both the MC3R and MC4R. As expected, homology modeling showed that D-Phe^7 in [Gln^6]α-MSH-ND could not contact the hydrophobic binding region of TM7, as observed in α-MSH-ND. Instead it adjoined to the residues of the TM3 domains in all three receptors. Compared to the altered binding sites of the MC3R (Ser^{122}) and MC4R (Ser^{127}), it was apparent that, in the MC1R, these Ser residues correspond to Val^{122}, which contains two methyl groups. Since the phenyl ring of [Gln^6]α-MSH-ND coincidentally overlaps with these two bulky groups, it is believed that its interaction with the valine residue of the MC1R, as opposed to the serine residue of either the MC3R or the MC4R, induces steric hindrance with the D-Phe^7 in the ligand. Furthermore, this repulsion interaction between these two residues results in the relatively low affinity of [Gln^6]α-MSH-ND to the MC1R.

Although this study has presented a strategy for developing a melanocortin analogue with minimized MC1R-selectivity, the potential optimal structure of the ligand contributing to MC3R or MC4R selectivity has not been elucidated. By homology modeling analysis, the binding pocket of the MC4R was determined to be narrower than that of either the MC1R or the MC3R. Other studies have also reported that the MC4R prefers cyclic ligands, whereas the MC1R and the MC3R are inclined to interact with linear species [27]. A ligand with a cyclic conformation tends to form a tight rigid structure. Therefore, it is likely that a fixed conformation of cyclic ligands is advantageous in terms of entering the narrow binding pocket of the MC4R, while the flexibility of linear ligands is best suited to cover the broad binding pockets of the MC1R and the MC3R.

In conclusion, the results of this study have suggested that minimizing MC1R activation simultaneously with preserving the comparable MC3R and MC4R selectivity may be achieved by modifying the D-Phe^7 side chain orientation of α-MSH-ND, while maintaining a 'type I β-turn'-like structure. In addition, the way the side chains of the α-MSH analogues interact with the melanocortin receptor subtypes was determined.

4. Significance

Many of the effects of melanocortin peptides are mediated via specific melanocortin receptor subtypes. Until now, most α-MSH analogues have not shown significant discrimination, and bind preferably to the MC1R, the MC3R and the MC4R with a high affinity. For this reason, the structural and functional analyses of the ligand–receptor interactions are essential for developing selective ligands to the specific melanocortin receptor subtypes, especially, to the MC3R and/or the MC4R. This report describes the biological activity of α-MSH-ND and the α-MSH-ND-derived analogues at the MC1R, the MC3R and the MC4R. Furthermore, it details the NMR structural characteristics, and demonstrates the interactions between the α-MSH analogues and the melanocortin receptor subtypes by receptor homology modeling analysis. The most significant finding was that [Gln^6]α-MSH-ND exhibits a type I′ β-turn, which is similar to the type I β-turn structure of α-MSH-ND. However, [Gln^6]α-MSH-ND had approximately 10 000 times less biological activity than α-MSH-ND at the MC1R, while the potencies of the two analogues were comparable at both the MC3R and the MC4R. These results can be explained by a structural difference in the side chain orientations of the sixth and seventh residues of [Gln^6]α-MSH-ND, which are mirror images of α-MSH-ND. The findings presented here suggest that minimizing MC1R selectivity whilst preserving the comparable potency for the MC3R and the MC4R may be achieved by modifying the D-Phe^7 orientation of

α-MSH-ND, while maintaining a 'type I β-turn'-like structure. These results will assist in understanding of the structure–activity relationships of the α-MSH analogues and provide a future direction for developing potent MC4R- and/or MC3R-selective α-MSH analogues.

5. Materials and methods

5.1. Chemicals

All media and sera for cell cultivation were purchased from Gibco-BRL (USA). The NDP-MSH and other chemicals were purchased from Sigma (USA), unless otherwise specified.

5.2. Peptide synthesis

The peptides used in this study were synthesized at the Korea Basic Science Institute (Seoul, South Korea) using the solid phase approach, and purified by high performance liquid chromatography (HPLC, Delta PAK 15 μ C18 300 Å 3.9 mm × 150 mm column, detection at 240 nm). Peptide sequences were assembled with a Milligen 9050 (Fmoc Chemistry), and peptide molecular weights were confirmed by mass spectroscopy. A reagent mixture (88% trifluoroacetic acid, 5% phenol, 2% triisopropylsilane, and 5% H_2O) was used for de-protection. The raw peptides formed were purified by HPLC.

5.3. Cell culture and stable transfections

The CHO cells were maintained in a F-12 medium (with glutamine) supplemented with 10% of fetal bovine serum, 100 units/ml penicillin G sodium, 100 μg/ml streptomycin sulfate and 0.25 μg/ml of amphotericin B. The cells were incubated in a 100-mm culture dish at 37°C in humidified air containing 5% CO_2. For transfections, the hMC1R, rMC3R and hMC4R cDNAs were cloned into the expression vector pcDNA I/neo. The cells were generally at 50% confluence on the day of transfection, this procedure being carried out using the calcium phosphate method, as described previously [15]. Briefly, the cells were fed with fresh complete culture medium containing 20 mM HEPES and incubated in a 95% air/5% CO_2 mixture. After 3–4 h, the medium was discarded and 5 ml of calcium phosphate–DNA precipitate containing 25 μg of DNA, 124 mM $CaCl_2$, 140 mM NaCl, 25 mM HEPES and 1.41 mM of Na_2HPO_4 (pH 7.12) was added. The cells were then incubated for 4 h in a 97% air/3% CO_2 mixture, washed with phosphate-buffered saline (PBS, 137 mM NaCl, 2.68 mM KCl, 4.3 mM N_2HPO_4, and 1.47 mM KH_2PO_4, at pH 7.12), and shocked with a glycerol buffer (15% glycerol, 140 mM NaCl, 25 mM HEPES and 1.41 mM Na_2HPO_4, at pH 7.12). The cells were again washed with PBS, and incubated for an additional 36–48 h in complete F-12 medium. They were then re-cultured in complete F-12 medium containing 0.5 mg/ml G418 (Geneticin; Life Technologies) until G418-resistant colonies were generated. The G418-resistant colonies were collected and subcultured for at least 10–14 days. Finally, the hMC1R-, rMC3R- and hMC4R-expressing cells were identified by screening more than 15 colonies and confirmed by assaying the NDP-MSH-induced cAMP accumulation.

5.4. Binding study

The iodinated NDP-MSH (the NDP-MSH sequence is Ser-Tyr-Ser-Ahx-Glu-His-Phe-Arg-Trp-Gly-Lys-Pro-Val), and the ^{125}I-(iodotyrosyl^2)-[Ahx^4, D-Phe^7]α-MSH, was prepared by a modification of chloramine-T method [15]. 1 mCi (10 μl) of $Na^{125}I$ (Amersham) was added to 5 μg of NDP-MSH in 100 μl of a 200 mM sodium phosphate buffer (pH 7.2). 20 μl of 2.8 mg/ml chloramine T solution in a 200 mM sodium phosphate (pH 7.2) was then added and the mixture allowed standing for 15 s, followed by the addition of 50 μl of 3.6 mg/ml of sodium metabisulfate to quench the reaction. The reaction mixture was diluted with 1 ml of 0.1% bovine serum albumin (BSA) solution containing 0.1% of trifluoroacetic acid and purified using a C18 Sep-Park cartridge (Waters) and Sephadex G25 gel filtration chromatography. The purified reagents were collected in 0.5-ml aliquots in Sigmacote-coated sterile glass tubes containing 100 μl of the PBS buffer with 0.1% BSA. For the binding assays, the stably transfected CHO cells were plated 48 h prior to the experiment in 24-well culture plates (Falcon Plastics) at a density of 5×10^4 per well until they were 90–95% confluent on the day of the assay. The maintenance media was removed and the cells were washed twice with washing buffer (50 mM Tris, 100 mM NaCl, 5 mM KCl, and 2 mM $CaCl_2$, at pH 7.2), then immediately incubated at 37°C for 2 h with 0.25 ml binding buffer per well (50 mM Tris, 100 mM NaCl, 5 mM KCl, 2 mM $CaCl_2$, 5% Hanks' balanced salt solution, and 0.5% BSA, at pH 7.2) containing 100 000 cpm (~2 nM) of [^{125}I]NDP-MSH and the appropriate concentrations of the unlabeled competing ligand. After incubation, the plates were placed on ice for 15 min, washed twice with 0.5 ml of an ice-cold binding buffer, and detached from the plates by twice flushing with 0.5 ml of 0.05 M NaOH (final volume: 1 ml). The radioactivity was then determined (Workman automatic γ counter) and the data analyzed with a software package suitable for radioligand binding data analysis (GraphPad Prism Program). Non-specific binding was determined by measuring the amount of bound [^{125}I]NDP-MSH remaining in the presence of 10^{-5} M unlabeled NDP-MSH, while the specific binding was calculated by subtracting the non-specifically bound radioactivity from the total bound radioactivity. The K_i (nM) values were calculated using the Cheng and Prusoff equation [28], and are reported as a mean ± S.E.M. All of the binding assays were performed in triplicate wells and repeated twice.

5.5. cAMP assay

The intracellular cAMP levels were determined using a previously described method [15]. The CHO cells over-expressing the MC1R, MC3R or MC4R were grown to 90–95% confluence in 24-well plates. The cell culture media were exchanged with complete F-12 medium containing 10% fetal bovine serum 3–4 h before the cells were treated with the peptides. For the assays, the media were removed and the cells were then washed with 0.5 ml of cAMP-generating medium (10% fetal bovine serum, 2 mM IBMX, 0.1% BSA, 20 mM HEPES, and 0.002% ascorbic acid in F-12 Medium). 0.25 ml of the cAMP-generating medium containing various peptide concentrations was added and the cells were incubated for 30 min at 37°C. At the completion of this incubation, the medium was completely discarded, and the cells were then frozen at −70°C for 30 min and thawed at room temper-

ature for 15–20 min, the freezing–thawing process was repeated twice. The cells were detached from the plates with 1 ml of a 50 mM HCl solution per well, transferred to a 1.5-ml Eppendorf tube, and then centrifuged at $1900 \times g$ for 10 min. The supernatants were diluted 50-fold with acetate buffer and the cAMP concentrations were measured using a cAMP ^{125}I RIA kit (Diasorin, USA), according to the assay instructions. The mean values of the collected data were fitted to a sigmoid curve with a variable slope factor by non-linear regression in a GraphPad Prism. The EC_{50} (nM) values are presented as a mean ± S.E.M. All the cAMP assays were performed in triplicate wells and repeated twice.

5.6. NMR experiments and structure determination

All NMR samples were prepared using the method described previously [14,15]. The NMR experiments were carried out at 10°C on a Bruker DRX-500 spectrometer equipped with a triple resonance probe with triple axis gradient coils. The NMR spectra were recorded over temperatures ranging from 5 to 25°C in order to calculate the temperature coefficients. Pulsed-field gradient (PFG) techniques were used for all H_2O experiments to suppress the solvent signals. 2D total correlation spectroscopy (TOCSY) with an MLEV-17 mixing pulse of 69.7 ms was then performed, as was the 2D nuclear Overhauser effect spectroscopy (NOESY) with mixing times of 100–600 ms. 2D rotating-frame Overhauser effect spectroscopy (ROESY) with 100–800-ms ROE mixing times was also performed in a D_2O solution. 2D double-quantum-filtered correlated spectroscopy (DQF-COSY) spectra were collected in H_2O to obtain the vicinal coupling constants. A series of 1D NMR measurements were obtained to identify the slowly exchanging amide hydrogen resonances in freshly prepared D_2O solutions after lyophilization of the H_2O sample. All NMR experiments were performed in the phase-sensitive mode using the time proportional phase incrementation (TPPI) method with 2048 data points in the t_2 and 256 in the t_1 domains. NMR data was processed using the XWIN-NMR (Bruker Instruments) software, and the processed data analyzed using the Sparky 3.60 software developed at UCSF on a Silicon Graphics Indigo^2 workstation. The initial structures were generated from distance geometry (DG) employing a refinement protocol described by Lee et al. [29]. The α-MSH-ND and [Gln^6]α-MSH-ND NOESY spectra yielded 47 and 58 NOE constraints, respectively. These distance restraints were assigned as strong, medium, or weak under the criterion of cross-peak volumes in the NOESY spectra. All categories had a lower limit of 1.8 Å, with upper limits of 2.7, 3.3, and 5.0 Å for strong, medium or weak intensities, respectively. The constraints for the dihedral angles of these peptides were also deduced on the basis of the $^3J_{HN\alpha}$ coupling constants from 2D DQF-COSY spectra in H_2O. The structure calculations were performed using hybrid DG and the dynamically simulated-annealing protocol with an X-PLOR 3.81 (Biosym/Molecular Simulations, Inc.) program on a Silicon Graphics Indigo^2 workstation.

5.7. Comparative modeling of MCRs

The TM regions of the receptor molecules were determined from both the sequence alignment and the topology prediction data of hMC1R, rMC3R and hMC4R [30,31]. The primary sequence alignment data was obtained from Haskell-Luevano et al. [32]. The molecular topology prediction of the receptors was performed using the Tosts method on an EMBL protein-predict server and this data was aligned with the bovine rhodopsin sequence. As bovine rhodopsin is one of the typical members of the G-protein coupled receptor families (GPCRs), which include the melanocortin receptors, it was selected as an excellent template of comparative modeling [33–35]. Initially, the MCR template structures were generated for only heavy atoms. Molecular models of the TM helix bundles were constructed with an orientation such that the helical axis was coincident with the corresponding axis in a modeled rhodopsin template [36]. These models were further refined by an energy minimization procedure. The force field used for the modeling calculations was cvff (definite cvff) in the Discover Module of the Insight II program (MSI Inc.) on a SGI Indigo^2 workstation. The 3D structures of the receptor molecules were completed by replacing the helical segments of the bovine rhodopsin with the melanocortin receptor sequences using the Modeler program [37]. This was followed by rearranging the helix orientations using the reported method [31].

After modeling, some correction criteria for the helix orientation were used to properly rearrange the TM sequences. First, previous reports on site-specific mutagenesis, which gives the information on the location of critical residues, were used. As discussed in the result section, Glu^{94}, Asp^{121}, Phe^{258}, and His^{260} should not face outward. Therefore, the TM sequences were rearranged to the template only in the range of 1 helix turn.

To validate the local structures of helices regions, the Eisenberg hydrophobic moment was calculated fitting the angles of the α-helix [38]. The hydrophobic interface should be located at 105 ± 15° on the axis of the helical wheel because a typical α-helix possesses 3.4 residues per turn. The most of individual segments of the TM regions were satisfied to this maximum hydropathy angle, but the TM4 regions were not. The sequence selection of the TM4 regions were based on a sequence alignment as well as a hydropathy plot, and no other data were available because these regions were not involved in the MSH activity. The unusual orientation of TM4 regions was considered as the effect of other helices, especially TM3. The unique axis of the TM3 helix may cause an interaction with its closest neighbor, TM4, and this interaction can have a synergistic effect beyond the sequence itself. Considering the research objectives, no further investigation into this region was required. However, the structural role of TM1, TM4 and TM5 regions, which are not involved in MSH activity, were studied.

Previous mutagenetic and biochemical data also provided information on the relative side chain orientations of the critical amino acids in the receptor molecule [23,39]. After all the coordinates were successfully arranged, a conformational search algorithm for the other side chains was performed using the side chain rotamer library. The final structures were evaluated with the PROCHECK program [40]. The TM residues in the allowed region of the Ramachandran plot were in 99.3% for the MC1R, 99.3% for the MC3R, and 100% for the MC4R. The overall *G*-factors were −0.4 for the MC1R, −0.37 for the MC3R, and −0.32 for the MC4R. The receptor–ligand complex structures of the MC1R, MC3R and MC4R were finally generated by a ligand docking procedure based on the mutagenetic and NMR data.

Acknowledgements

This work was supported by research Grants from the Korean Ministry of Health and Welfare (HMP-98-D-4-0033) (1998) and Brain Korea 21 Project for Medical Sciences. We thank Dr. Roger. D. Cone (Vollum Institute for Advanced Biomedical Research, Portland, OR, USA) for kindly supplying the rMC3R and hMC4R cDNA and Dr. Ira Gantz (Department of Surgery, University of Michigan Medical Center, Ann Arbor, MI, USA) for kindly providing the hMC1R cDNA. We also thank Dr. John Roberts for English language revision.

References

[1] G. Ceriani, A. Macalus, A. Catania, J.M. Lipton, Central neurogenic antiinflammatory action of α-MSH, Neuroendocrinology 59 (1993) 138–143.

[2] P. Van Bergen, P.M. Janssen, P. Hoogerhout, D.J. De Wildt, D.H. Versteeg, Cardiovascular effects of γ-MSH/ACTH-like peptides: structure–activity relationship, Eur. J. Pharmacol. 294 (1995) 795–803.

[3] D. De Wied, Inhibitory effects of ACTH and related peptides on extinction of conditioned avoidance behavior in rats, Proc. Soc. Exp. Biol. Med. 122 (1966) 28–32.

[4] W. Fan, B.A. Boston, R.A. Kesterson, V.J. Hruby, R.D. Cone, Role of melanocortinergic neurons in feeding and the *agouti* obesity syndrome, Nature 385 (1997) 165–168.

[5] P.C. Contreras, A.E. Takemori, Antagonism of morphine-induced analgesia, tolerance and dependence by α-MSH, J. Pharmacol. Exp. Ther. 229 (1984) 21–26.

[6] E.M. Smith, T.K. Hughes, F. Hashemi, G.B. Stefano, Immunosuppressive effects of corticotropin and melanotropin and their possible significance in human immunodeficiency virus infection, Proc. Natl. Acad. Sci. USA 89 (1992) 782–786.

[7] V. Chhajlani, R. Muceniece, J.E.S. Wikberg, Molecular cloning and expression of the human melanocyte stimulating hormone receptor, Biochem. Biophys. Res. Commun. 195 (1993) 866–873.

[8] V. Chhajlani, J.E.S. Wikberg, The cloning of a family of genes that encode the melanocortin receptors, FEBS Lett. 309 (1992) 417–420.

[9] I. Gantz, Y. Konda, T. Tashiro, Y. Shimoto, H. Miwa, G. Munzert, S.J. Watson, J. DelValle, T. Yamada, Molecular cloning of a novel melanocortin receptor, J. Biol. Chem. 268 (1993) 8246–8250.

[10] I. Gantz, H. Miwa, Y. Konda, Y. Shimoto, T. Tashiro, S.J. Watson, J. DelValle, T. Yamada, Molecular cloning, expression and gene localization of a fourth melanocortin receptor, J. Biol. Chem. 268 (1993) 15174–15179.

[11] K.G. Mountjoy, L.S. Robbins, T.T. Mortrud, R.D. Cone, The cloning of a family of genes that encode the melanocortin receptors, Science 257 (1992) 1248–1251.

[12] K.G. Mountjoy, J. Wong, Obesity, diabetes and functions for proopiomelanocortin-derived peptides, Mol. Cell. Endocrinol. 128 (1997) 171–177.

[13] J.E.S. Wikberg, Melanocortin receptors: perspectives for novel drugs, Eur. J. Pharmacol. 375 (1999) 295–310.

[14] J.H. Lee, S.K. Lim, S.H. Huh, D. Lee, W. Lee, Solution structures of the melanocyte-stimulating hormones by two-dimensional NMR spectroscopy and dynamical simulated-annealing calculation, Eur. J. Biochem. 257 (1998) 31–40.

[15] S.Z. Li, J.H. Lee, W. Lee, C.J. Yoon, J.H. Baik, S.K. Lim, Type I β-turn conformation is important for biological activity of the melanocyte-stimulating hormone analogues, Eur. J. Biochem. 265 (1999) 430–440.

[16] H.I. Mosber, J.R. Omnaas, A. Lomize, D.L. Hey, I. Nordan, C. Mousigian, P. Davis, F. Porreca, Development of a model for the delta opioid receptor pharmacophore. 2. Conformationally restricted Phe3 replacements in the cyclic delta receptor selective tetrapeptide Tyr-c[D-Cys-Phe-D-Pen]OH (JOM-13), J. Med. Chem. 37 (1994) 4384–4391.

[17] F.D. Lung, J.P. Meyer, G. Li, B.S. Lou, D. Stropove, T. Davis, F. Porreca, H.I. Yamamura, V.J. Hruby, Highly kappa receptor-selective dynorphin A analogues with modifications in position 3 of dynorphin A(1-11)-NH2, J. Med. Chem. 38 (1995) 585–586.

[18] B.Y. Azizeh, M.D. Shenderovich, D. Trivedi, G. Li, N.S. Sturm, V.J. Hruby, Topographical amino acid substitution in position 10 of glucagon leads to antagonists/partial agonists with greater binding differences, J. Med. Chem. 39 (1996) 2449–2455.

[19] M. Lebl, G. Toth, J. Slaninova, V.J. hruby, Conformationally biased analogs of oxytocin, Int. J. Pept. Protein Res. 40 (1992) 148–151.

[20] K.E. Köver, D. Jiao, S. Fang, V.J. Hruby, Conformational analysis of four β-methylphenylalanine stereoisomers in a bioactive peptide by *z*-filtered relay NMR spectroscopy, Magn. Reson. Chem. 31 (1993) 1072–1076.

[21] Z. Huang, Y. He, K. Raynor, M. Tallent, T. Reisine, M. Goodman, Main chain and side chain chiral methylated somatostatin analogues: syntheses and conformation analyses, J. Am. Chem. Soc. 114 (1992) 9390–9401.

[22] C. Haskell-Luevano, K. Toth, L. Boteju, C. Job, A.M.L. Castrucci, M.E. Hadley, V.J. Hruby, Beta-Methylation of the Phe7 and Trp9 melanotropin side chain pharmacophores affects ligand–receptor interactions and prolonged biological activity, J. Med. Chem. 40 (1997) 2740–2749.

[23] Y.K. Yang, C. Dickinson, C. Haskell-Luvano, I. Gantz, Molecular basis for the interaction of [Nle^4, D-Phe^7]melanocyte-stimulating hormone with the human melanocortin-1 receptor, J. Biol. Chem. 272 (1997) 23000–23010.

[24] P.-A. Frändberg, X. Xu, V. Chhajlani, Glutamine235 and arginine272 in human melanocortin 5 receptor determines its low affinity to MSH, Biochem. Biophys. Res. Commun. 236 (1997) 489–492.

[25] H.B. Schiöth, R. Muceniece, M. Larsson, F. Mutulis, M. Szardenings, P. Prusis, G. Lindeberg, J.E.S. Wikberg, Characterization of D117A and H260A mutations in the melanocortin 1 receptor, Mol. Cell. Endocrinol. 125 (1997) 213–219.

[26] H.B. Schiöth, R. Muceniece, M. Szardenings, P. Prusis, J.E.S. Wikberg, Evidence indicating that the TM4, EL2, and TM5 of the melanocortin 3 receptor do not participate in ligand binding, Biochem. Biophys. Res. Commun. 229 (1996) 687–692.

[27] T.K. Sawyer, V.J. Hruby, P.S. Darman, M.E. Hadley, [Half-Cys4, half-Cys10]-alpha-Melanocyte-stimulating hormone: a cyclic alpha-melanotropin exhibiting superagonist biological activity, Proc. Natl. Acad. Sci. USA 79 (1982) 1751–1755.

[28] Y. Cheng, W.H. Prusoff, Relationship between the inhibition constant(K_i) and the concentration of inhibitor which causes 50 percent inhibition (IC_{50}) of an enzymatic reaction, Biochem. Pharmacol. 22 (1973) 3099–3108.

[29] W. Lee, C.H. Moore, D.D. Watt, N.R. Krishina, Solution structure of the variant-3 neurotoxin from *Centruroides sculpturatus* Ewing, Eur. J. Biochem. 218 (1994) 89–95.

[30] R.A.H. Adan, W.H. Gispen, Brain melanocortin receptors: from cloning to function, Peptides 18 (1997) 1279–1287.

[31] D. Eisenberg, E. Schwarz, M. Komaromy, R. Wall, Analysis of membrane and surface protein sequences with the hydrophobic moment plot, J. Mol. Biol. 179 (1984) 125–142.

[32] C. Haskell-Luevano, S. Hendrata, C. North, T.K. Sawyer, M.E. Hadley, V.J. Hruby, C. Dickinson, I. Gantz, Discovery of prototype peptidomimetic agonists at the human melanocortin receptors MC1R and MC4R, J. Med. Chem. 40 (1997) 2123–2129.

[33] D. Strahs, H. Weinstein, Comparative modeling and molecular dynamics studies of the δ, κ and μ opioid receptors, Protein Eng. 10 (1997) 1019–1038.
[34] Z. Lin, A. Shenker, R. Pearlstein, A model of the lutropin/choriogonadotropin receptor: insights into the structural and functional effects of constitutively activating mutations, Protein Eng. 10 (1997) 501–510.
[35] C. Labbe-Jullie, S. Barroso, D. Nicolas-Eteve, J.L. Reversat, J.M. Botto, J. Mazella, J.M. Bernassau, P. Kitabgi, Mutagenesis and modeling of the neurotensin receptor NTR1. Identification of residues that are critical for binding SR 48692, a nonpeptide neurotensin antagonist, J. Biol. Chem. 273 (1998) 16351–16357.
[36] J.M. Baldwin, F.X.G. Schertler, V.M. Unger, An alpha-carbon template for the transmembrane helices in the rhodopsin family of G-protein-coupled receptors, J. Mol. Biol. 272 (1997) 144–164.
[37] A. Sali, T.L. Blundell, Comparative protein modeling by satisfaction of spatial restraints, J. Mol. Biol. 234 (1993) 779–815.
[38] D. Eisenberg, E. Schwarz, M. Komaromy, R. Wall, Analysis of membrane and surface protein sequences with the hydrophobic moment plot, J. Mol. Biol. 179 (1984) 125–142.
[39] P. Prusis, P.A. Frandberg, R. Muceniece, I. Kalvinsh, A three-dimensional model for the interaction of MSH with the melanocortin-1 receptor, Biochem. Biophys. Res. Commun. 210 (1995) 205–210.
[40] R.A. Laskowski, M.W. MacArthur, D.S. Moss, J.M. Thornton, PROCHECK: a program to check the stereochemical quality of protein structures, J. Appl. Crystallogr. 26 (1993) 47–60.